Available online www.jocpr.com

Journal of Chemical and Pharmaceutical Research, 2015, 7(3):44-55

Research Article

ISSN : 0975-7384
CODEN(USA) : JCPRC5

Synthesis, biological activity and theoretical study of some isatin, and their metal complexes

Fatma Kandemirli[a*], Saima Rasheed[b], Hakan Sezgin Sayiner[c], Yusuf Akkaya[d], Can Dogan Vurdu[a] and M. Iqbal Choudhary[b,e]

[a]*Department of Biomedical Engineering, Faculty of Engineering and Architecture, Kastamonu University, Kastamonu, Turkey*
[b]*H. E. J. Research Institute of Chemistry, International Center for Chemical and Biological Sciences, University of Karachi, Karachi, Pakistan*
[c]*Medical Faculty, Adiyaman Üniversitesi, Adiyaman, Turkey*
[d]*Department of Chemistry, Faculty of Science, Nigde University, Nigde, Turkey*
[e]*Department of Biochemistry, Faculty of Science, King Abdulaziz University, Jeddah, Saudi Arabia*

ABSTRACT

*Isatin thiosemicarbazone and its metal complexes have been prepared and structurally characterized by elemental analyses and FT-IR, electronic and ^{1}H-NMR, ^{13}C-NMR spectra. The theoretical wavenumbers, IR intensities, ^{1}H-NMR, ^{13}C-NMR spectroscopy, UV absorption spectra and and molecular parameters were calculated by the B3LYP method. Frontier molecular orbital energies, bond length and charges on the atoms of I4NPTH$_2$ and I2-4CPTH$_2$ were studied by the B3LYP method using 6-31G (d,p), 6-311G (d,p), 6-311++G (d,p), 6-311++G (2d,2p)basis sets in gas and DMSO phases. Results showed that compounds **8**, **10** and **5** are potent inhibitors of in vitro protein glycation with IC$_{50}$ value of 111.30 ± 1.96, 113.00 ± 0.9 and 161.51 ± 0.47 µM, respectively While compounds **1**- **4** were found to be inactive.*

Keywords: Isatin, Metal complexes, Thiosemicarbazone, Anti-glycation

---

INTRODUCTION

Isatin (indole-2,3-dione), which is an endogenous compound, is widely distributed in mammalian tissues and body fluids, and is well known as pharmacological agent with activity against certain types of infections [1]. Isatin (1*H*-indole-2,3-dione) attracted a major interest among indole derivatives. It is a general starting material for the preparation of versatile heterocyclic compounds. Isatin (1*H*-indole-2,3-dione) and its derivatives reported to have activities such as inhibition of monoamine oxidase, anti-bacterial, anti-fungal, anti-viral, anti- HIV, anti-allergic, anti-protozoal, muscle relaxant, and anti-inflammatory properties [2-10].

We previously reported the spectroscopic and theoretical properties on 5-fluoroisatin-3-(*N*-benzylthiosemicarbazone) (H2FLB) and its Zn(II) complex [11], 5-methoxyisatin-3-(N-(4-cyclohexyl)) thiosemicarbazone ligand (H2MICT) and its coordination with Ni(II), and Zn(II) [12], and 5-methoxyisatin, 5-fluoroisatin -derivatives [9,14] and *bis*(fluoroisatinato)mercury(II) (Hg(FI)$_2$[15].

In this study, *I4NPTH$_2$, I4IPTH$_2$, I2-4CPTH$_2$, Zn[(I4NPTH)$_2$], Zn[(I4IPTH)$_2$] , Zn[(I2-4CPTH)$_2$], Ni[(I4NPTH)$_2$], Ni[(I4IPTH)$_2$], Co[(I4NPTH)$_2$], Ni[(I2-4CPTH)$_2$]* and *Ni[(I2FPTH)$_2$]* were synthesized and characterized with elemental analysis, and IR, UV, and ^{1}H-NMR spectroscopic analysis. Besides, density functional theory (DFT) by using B3LYP hybrid functionals and *ab initio* Hartree–Fock (HF) computations with the 3-21G, 3-21G*, 6-31G(d,p), 6-311G (d,p), 6-311++G (d,p), 6-311++G (2d,2p), basis sets, the vibrational spectrum, UV spectrum, ^{13}C

NMR , ^{1}H NMR values, the molecular geometry, the atomic charges and molecular polarizability were also predicted, Fukui functions were also calculated by using AOMix [16,17] from single-point calculations with B3LYP/6-311G(d,p) [18].

Glycation is a non enzymatic chemical transformation in which biomolecules such as proteins, human DNA, and lipids are damaged by the attack of reducing sugars (e.g. glucose). This process finally leads to the formation of highly reactive Advanced Glycation Endproducts (AGEs), which are associated with deleterious health effects. Protein glycation has been implicated in the development of pathologies associated with diabetes, ageing, etc. Therefore efforts have now been made to explore new and safe anti-glycation agents in order to prevent the formation of AGEs (e.g. free radicals, dicarbonyl species, protein cross-links, etc.) [19].

In continuation of our studies on anti-glycation agents, we are reporting here the anti-glycation activity of isatins and their metal complexes.

EXPERIMENTAL SECTION

2.1. Material and Instrument*:*

FT-IR Spectra were recorded by using JASCO 300 FT-IR in the region 4000–400 cm^{-1}. Melting points were determined on Electrothermal 9100 apparatus and are uncorrected. The elemental analysis was carried out on CHNS-932 (LECO) and ^{1}H NMR spectra were recorded on Bruker DPX-400 ultrashield. Bovine serum albumin (BSA) was purchased from Merck Marker Pvt. Ltd. (Germany), lysozyme (chicken egg white) was purchased from Bio Basic Inc. (Canada), rutin and methylglyoxal (MG) (40% aqueous solution) were from Sigma Aldrich (USA), and sodium dihydrogen phosphate (NaH_2PO_4), disodium hydrogen phosphate (Na_2HPO_4) and sodium azide (NaN_3) were obtained from Scharlau Chemie, S. A. (Spain). Dimethyl sulphoxide (DMSO) was purchased from Fisher Scientific (UK).

2.2. Chemistry and General Methods

1*H*-indole-2,3-dione 3-(4-nitrophenyl)thiosemicarbazone)

A solution of 4-(4-nitrophenyl-3-thiosemicarbazide in ethanol was added to a solution of isatin in ethanol. A drop of conc. H_2SO_4 was added to the mixture and refluxed for 2-3 h. After cooling, orange solid was filtered and washed with ethanol or methanol, m.p: 266° C, (Calculated: % C: 52.78, % H: 3.25, % N: 20.52, % S: 9.39; Found: % C: 52.81, % H: 3.12, % N: 20.49, % S: 9.02)

1*H*-indole-2,3-dione 3-(4 iodophenyl)thiosemicarbazone)

0.294 g of 1*H*-indole-2,3-dione ($C_9H_7NO_3$) in 50 mL ethanol was heated in a water bath until it was dissolved. To this solution, 0.5222 g of 4-(4-iodophenyl)-3-thiosemicarbazide ($C_7H_8N_4O_2S$) dissolved in ethanol was added dropwise, then a drop of conc. H_2SO_4 was added to the mixture and refluxed for 2-3 h. After cooling resulting red color solid was filtered and washed with ethanol and petroleum ether, m.p: 259° C, (Calculated: % C: 42.67, % H: 2.62, % N: 13.27, % S: 7.59; Found: % C: 42.57, % H: 2.62, % N: 13.17, % S: 6.94)

1*H*-indole-2,3-dione 3-(2,4 dichlorophenyl)thiosemicarbazone)

A solution of 4-(2-4 dichlorophenyl-3-thiosemicarbazide in ethanol was added to a solution of isatin in ethanol. A drop of conc. H_2SO_4 was then added to the mixture and refluxed for 2-3 h. After cooling, resulting orange solid was filtered and recrystalized with ethanol or methanol (m. p.: 266 $^\circ$C). (Calculated: % C: 52.78, % H: 3.25, % N: 20.52, % S: 9.39; Found: % C: 52.81, % H: 3.12, % N: 20.49, % S: 9.02)

***Bis*(isatin-3-(*N*-4- nitrorophenyl) thiosemicarbazonato)zinc(II) complex Zn**

1 mmol (0.34126 g) of "1*H*-indole-2,3-dione 3-(4 iodophenyl)thiosemicarbazone)" was dissolved in 20 mL of methanol at 50-55 ºC and then slowly methanol solution (10 mL) of 0.5 mmol (0.1097 g) zinc acetate tetradehydrate was added. The mixture was refluxed for 6-9 h. Dark orange product was precipitated during the reaction, which was washed with ethanol and diethylether, and then dried (m. p.: 277º C). (Calculated: % C: 48.29, % H: 2.70, % N: 18.74, % S: 8.59; found: % C: 47.34, % H: 3.56, % N: 17.73, % S: 8.58).

***Bis*(isatin-3-(4-iodophenyl)thiosemicarbazonato)zinc(II)Zn**

1 mmol (0.4221 g) of "1*H*-indole-2,3-dione 3-(4 iodophenyl)thiosemicarbazone)" was dissolved in 15 mL of ethanol at 50-55 ºC and was then slowly methanol solution (10 mL) of 0.5 mmol (0.1097 g) zinc acetate tetradehydrate was added. The mixture was refluxed for 6-9 h at a temperature of approximately dark orange product was precipitated during the reaction, which was washed with ethanol and diethylether, and then dried (m. p.: 292º C). (calculated: % C: 39.69, % H: 2.22, % N: 12.34, % S:7.06; found: % C: 39.37, % H: 2.28, % N: 12.15, % S:6.18).

***Bis*(isatin-3-(2,4-dichlorophenyl)thiosemicarbazonato)zinc(II)**
1mmol (0.3661 g) of *I2-4CPTH*$_2$ was dissolved in 15 mL of methanol at 50-55 ºC and then slowly methanol solution (10 mL) of 0.5 mmol (0.1097 g) zinc acetate tetradehydrate was added. The mixture was refluxed for 6-9 h. Dark orange product precipitated during the reaction, was washed with ethanol and diethylether, and then dried. (m. p.: 305º C). (calculated: % C: 45.39, % H: 2.28, % N: 14.11, % S: 8.07; found: % C: 45.08, % H: 2.42, % N:13.72, % S: 7.04).

***Bis*(isatin-3-(4-nitrophenyl)thiosemicarbazonato)nickel(II) (7)**
1 mmol (0.34126 g) of *I4NPTH*$_2$ was dissolved in 20 mL of methanol at 50-55 ºC and then slowly methanol solution (15 mL) of 0.5 mmol (0.1244 g) nickel acetate tetradehydrate wad added. The mixture was refluxed for 2 h, and stirred for two days at room temperature. Brown product, precipitated during the reaction, was washed with ethanol and diethylether, and then dried (m. p.: 309º C). (calculated: % C:48.30, % H:2.93, % N: 18.18, % S: 8.02; found: % C: 47.34, % H: 2.93, % N: 17.73, % S:8.58).

***Bis*(isatin-3-(4- iodophenyl)thiosemicarbazonato)nickel(II) (8)**
1 mmol (0.293 g) of *I4NPTH*$_2$. was dissolved in 15 mL of ethanol at 50-55 ºC and then slowly methanol solution (15 mL) of 0.5 mmol (0.1244 g) nickel acetate tetradehydrate was added. The mixture was refluxed for 2 h and stirred for two days at room temperature. Orange product was precipitated during the reaction, which was washed with ethanol and diethylether, and then dried (m. p.: 323º C). (Calculated: % C: 39.98, % H: 2.24, % N: 12.43, % S: 7.11; found: % C: 39.37, % H: 2.28, % N: 12.15, % S: 6.17).

***Bis*(isatin-3-(4-nitrophenyl)thiosemicarbazonato) cobalt(II) (9)**
1 mmol (0.34 g) of *I4NPTH*$_2$ was dissolved in 15 mL of ethanol at 50-55 ºC and then slowly methanol solution (15 ml) of 0.5 mmol (0.1245 g) cobalt acetate tetradehydrate was added. The mixture was refluxed for 2 h. Brown product was precipitated during the reaction, which was washed with ethanol and diethylether, and then dried (m. p.: 293 ºC) (Calculated: % C: 48.72, % H: 2.72, % N: 18.94, % S: 8.67; found: % C: 47.75, % H: 2.99, % N: 18.28, % S: 8.89).

***Bis*(isatin-3-(2,4-dichlorophenyl)thiosemicarbazonato)nickel(II) (10)**
1 mmol (0.236 g) of *I2-4CPTH*$_2$ was dissolved in 15 mL of ethanol at 50-55 ºC and was then slowly methanol solution (15 mL) of 0.5 mmol (0.1244 g) nickel acetate tetradehydrate was added. The mixture was refluxed for 2 h and stirred for two days at room temperature. Orange product was precipitated during the reaction, which was washed with ethanol and diethylether, and then dried (m. p.: 312º C). (Calculated: % C: 45.77, % H: 2.30, % N: 14.24, % C: 44.21, % H: 2.04, % N: 13.71.

Bis(isatin-3-(2-florophenyl)thiosemicarbazonato)nickel(II) (11)
1 mmol of *I2FTH*$_2$ (0.3142 g) was dissolved in 20 mL of methanol at 50-55 ºC and then slowly methanol solution (15 mL) of 0.5 mmol (0.1244 g) nickel acetate tetradehydrate was added. The mixture was refluxed for 2 h and stirred for two days at room temperature. Brown product, precipitated during the reaction, was washed with ethanol and diethylether, then dried (m. p: 312º C). (Calculated: % C: 52.57, % H: 2.94, % N: 15.91, % S: 9.35; found: % C: 51.66, % H: 2.92, % N: 15.91, % S: 8.98).

2.3. Theoretical Calculations
Quantum chemical calculations were performed with the DFT level of theory with the three parameter Becke-style hybrid functional (B3LYP), which employs the Becke exchange and LYP correlation functionals and RHF level of theory. The Gaussian basis sets 3-21G, 3-21G*, 6-31G (d,p), 6-311G (d,p), 6-311++G (d,p), 6-311++G (2d,2p) were used for geometry optimizations. All the calculations were performed by using the software package of Gaussian-09 [20]. Excitation energies and oscillator strengths for UV spectra of *I4NPTH*$_2$, *I2-4CPTH*$_2$ *and* n[(I4NPTH)$_2$] complex were calculated by using TDDFT within GAUSSIAN09.

2.4. *In Vitro* BSA-MG Anti-Glycation Assay
The total reaction volume of the assay was 200 µL (having final concentrations of 10 mg/mL BSA, 14 mM methylglyoxal, and 1 mM test compounds). 10 mg/mL solution of BSA and 14 mM methylglyoxal was prepared in 0.1 M phosphate buffer (pH 7.4), containing sodium azide (NaN_3) (3 mM) as antimicrobial agent, while solutions of test compounds were prepared in the DMSO (final concentration 10%). Assay was performed in triplicate in 96-well plate; reaction mixture in each well comprised of 50 µL BSA, 50 µL methylglyoxal, 20 µL test compound and 80 µL phosphate buffer (pH 7.4). The reaction mixture was incubated under aseptic conditions at 37 °C for 9 days.
After completion of nine days of incubation, each sample was examined for the development of specific fluorescence (excitation 330 nm; emission 420 nm) against blank on a microtitre plate reader (SpectraMax M2, Molecular Devices, CA, USA) [21, 22].

The percent inhibition of AGE formation by the test sample was calculated by using the following formula:

% Inhibition= (1− Fluorescence of test sample/ Fluorescence of the control) × 100

2.5. Software Used/Statistical Analysis

All experiments were performed in 96-well microplate reader (SpectraMax M2, Molecular Devices, CA, USA). The obtained results were analyzed by SoftMaxPro 4.8 and MS-Excel. Results are presented as means ± SEM from three experiments. IC_{50} Values were determined by using EZ-FIT, Enzyme kinetics software by Perrella Scientific, Inc., USA.

RESULTS AND DISCUSSION

3.1 Chemistry and Geometric Parameters

The labeling of the atoms *I4NPTH$_2$, I2-4CPTH$_2$ ligands and* Zn[(I4NPTH)$_2$] complex by using DFT method at the B3LYP/6-31G(d) level is shown in Fig. 1.

The Frontier energy energies of BMC *I4NPTH$_2$* were deduced using the DFT method with the 6-31G(d,p), 6-311G(d,p), 6-311++G(d,p), 6-311G(2d,2p) basis sets in gas phase and DMSO as shown in Fig. 6. The knowledge about E_{HOMO} and E_{LUMO} is important for the better understanding of their fluorescence. It was observed that E_{HOMO} and E_{LUMO} values, calculated with DMSO, were smaller than he values calculated at gas phase. E_{HOMO} Values of *I4NPTH$_2$* were calculated in gas phase by using 6-31G (d,p), 6-311G (d,p), 6-311++G (d,p), 6-311G(2d,2p) basis sets are -0.23154 au, -0.23913 au, -0.24337 au, -0.24163 au; in DMSO are -0.22399 au, -0.23113 au, -0.23456 au, -0.23337 au; and E_{LUMO} values are -0.10841 au, -0.11579 au, -0.12162 au, -0.12055 au in gas phase and are -0.10366 au, -0.11024 au, -0.11810 au, -0.11660au in DMSO.

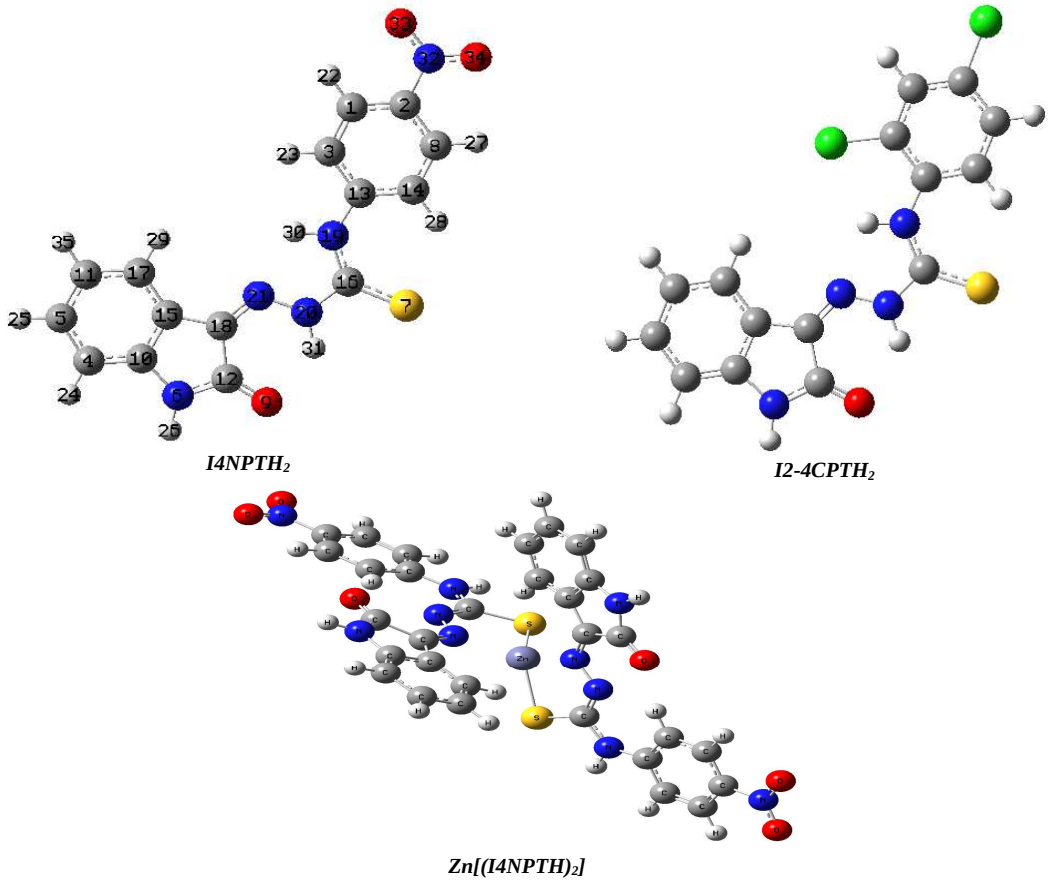

I4NPTH$_2$ ***I2-4CPTH$_2$***

Zn[(I4NPTH)$_2$]

Figure-1: Geometry of *I4NPTH$_2$, I2-4CPTH$_2$ and* Zn[(I4NPTH)$_2$] optimized at the B3LYP/6-311G(d,p) level

E_{HOMO} Values of *I2-4CPTH$_2$*, calculated in gas phase by using 6-31G(d,p), 6-311G(d,p), 6-311++G(d,p), 6-311G(2d,2p) basis sets, were 0.22436 au, -0.23260 au, -0.23515 au, -0.23399 au; in DMSO are -0.22306 au, -0.23040 au, -0.23350 au, -0.23220 au; and E_{LUMO} values are 0.09998 au, -0.10809au, -0.11241 au, -0.11140 au in gas phase and are -0.09718 au, -0.10413 au, -0.10848 au, -0.10732 au in DMSO. HOMO Energy of *I4NPTH$_2$* ligand is smaller than that of *I2-4CPTH$_2$* ligand calculated for all basis sets.

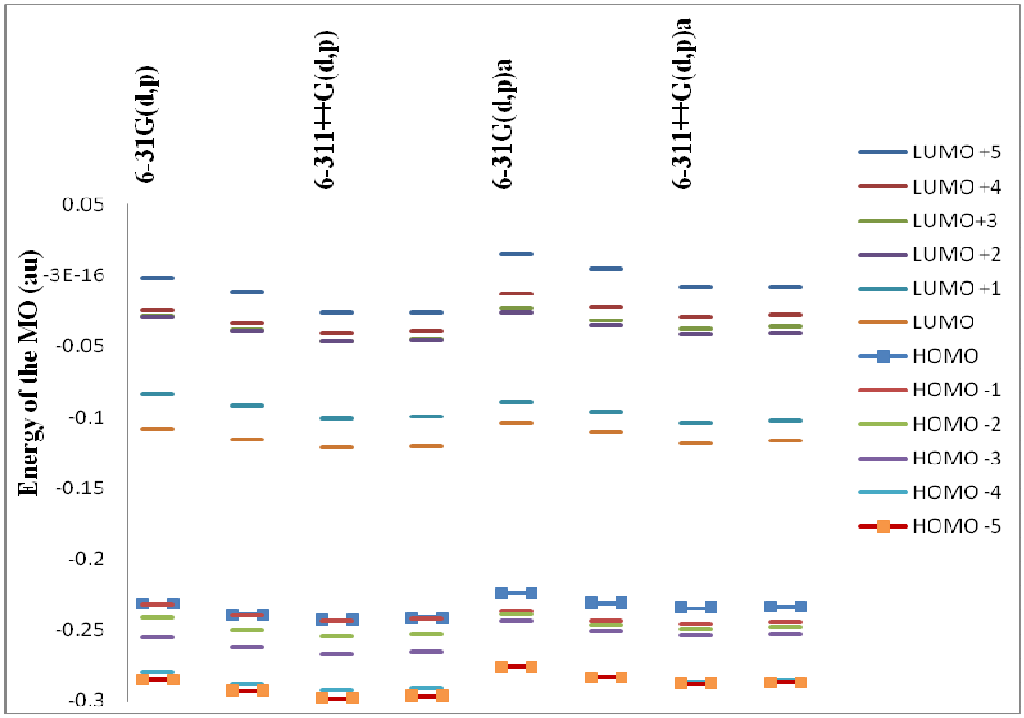

Figure-2: Frontier Molecular Orbital Energies of *I4NPTH₂*

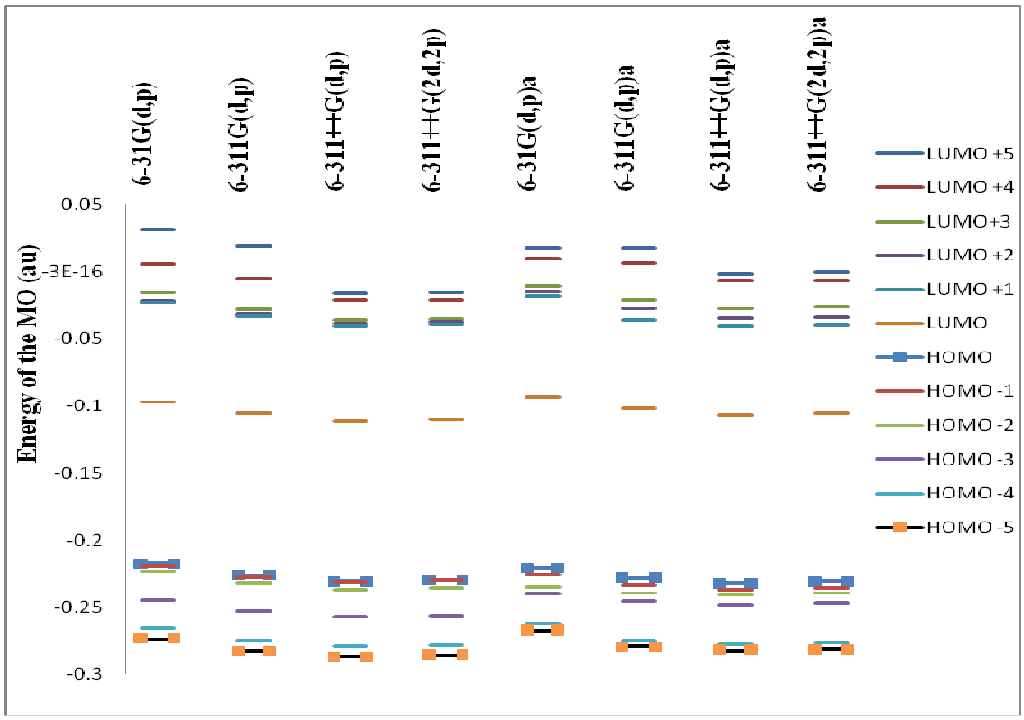

Figure-3: Frontier Molecular Orbital Energies of *I2-4CPTH₂*

Mulliken charges of the selected atoms, calculated with B3LYP/6-311G(d,p) for $I4NPTH_2$, $I2\text{-}4DKPTH_2$ ligands and $Zn[(I4NPTH)_2]$ complex, are presented in Fig. 4 and bond lengths are shown in Fig, 5.

Mulliken charges provide a means of estimating partial atomic charges. C11, C5, C4, C15, N6, O9, N21, N20, S7, N19 of $I4NPTH_2$, $I2\text{-}4DKPTH_2$ ligands and $Zn[(I4NPTH)_2]$ complex possess negative charges, while C10, C12, C18, C16, C13ahave positive charges. Mulliken charge of C17 was -0.024 ē, -0.020 ē, 0.036 ē. Mulliken charge of C-18 atom belonging to indole ring, and N21, N20, C16, and S7 atoms belonging to thiosemicarbazone group were 0.099 ē, -0.244 ē, -0.270 ē, 0.228 ē, -0.186 ē. while in the $Zn[(I4NPTH)_2]$ complex, 0.212 ē, -0.538 ē, -0.218 ē, 0.164 ē, -0.421 ē. Bond lengths of the C18-N21, N21-N20, N20-C16, C16-S7, C16-N19 were found to 1.295 Å,

1.336 Å, 1.391 Å, 1.666 Å, and 1.360 Å; for I4NPTH$_2$ ligand, 1.294 Å, 1.335 Å, 1.391 Å, 1.669 Å, 1.358 Å and for I2-4DKPTH2 ligand, 1.308Å, 1.352 Å, 1.320 Å, 1.755 Å, and 1.369 Å, respectively.

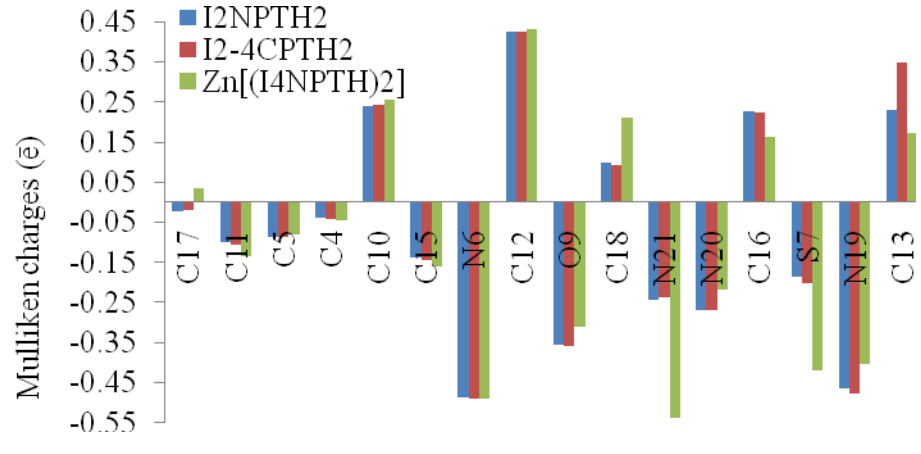

Figure-4: Mulliken charge of I4NPTH$_2$, I2-4DKPTH$_2$ ligands and Zn[(I4NPTH)$_2$] complex

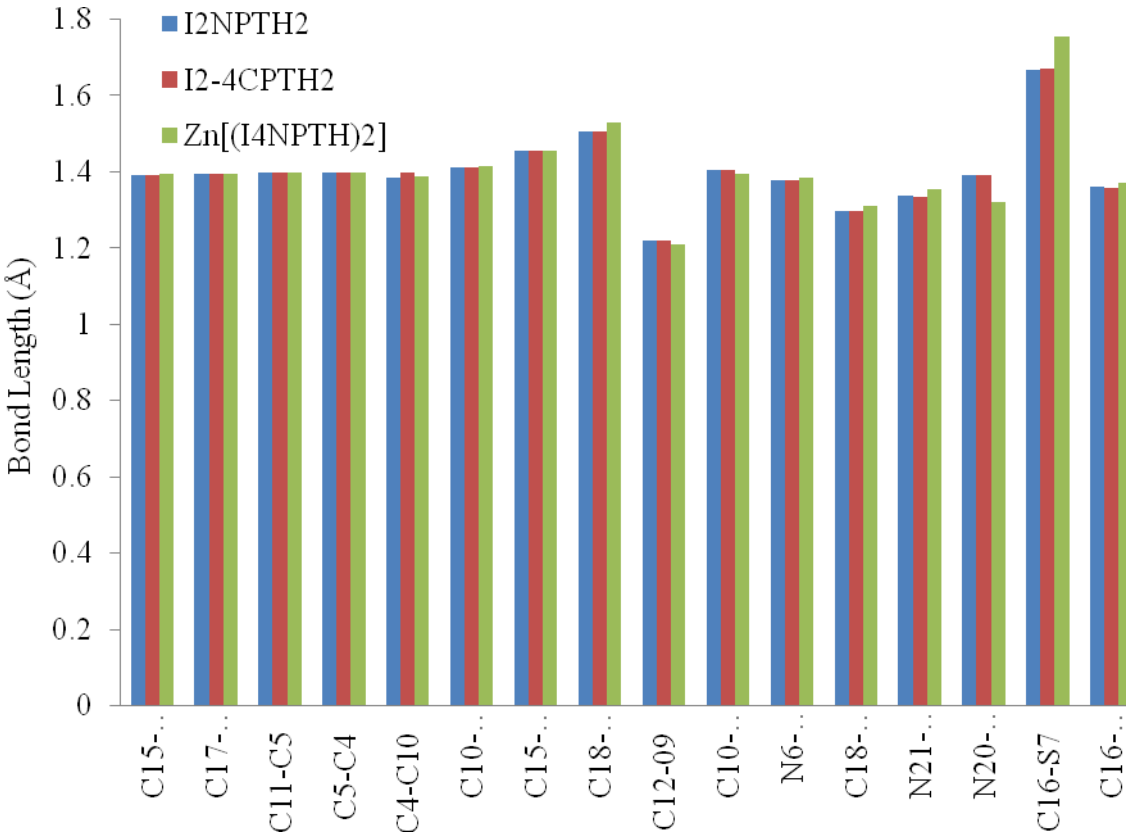

Figure-5: Bond length of I4NPTH$_2$, I2-4DKPTH$_2$ ligands and Zn[(I4NPTH)$_2$] complex

3.2 Fukui Functions:

AOMix Program [16, 17] was used to calculate the Fukui indices. Fukui functions provide information about which atoms in a molecule have a larger tendency to either loose or accept an electron. This allows to evaluate the nucleophilic and electrophilic behaviors of each atom in the molecule. Fukui functions can be expressed by the following equations:

$f_k^+ = \rho_k(N+1) - \rho_k(N)$ (for nucleophilic attack)

$f_k^- = \rho_k(N) - \rho_k(N-1)$ (for electrophilic attack)

where *k* represents the sites (atoms / molecular fragments) for nucleophilic, electrophilic and radical agents, and ρ_k represents gross electron populations. An elevated value of f_k implies a high reactivity of the site *k*. The values

of the Fukui functions of *I4NPTH$_2$*, *I2FPTH$_2$*, *I2-4CPTH$_2$*, ligands calculated by B3LYP/6-31G (d,p) and B3LYP/6-31G (d,p), are presented in Table 1 (The values smaller than 3 is not included in the Table-1).

Table-1: Fukui functions of *I4NPTH$_2$*, *I2FPTH$_2$*, *I2-4CPTH$_2$*

	I4NPTH$_2$		*I2-4CPTH$_2$*			*I4NPTH$_2$*		*I2-4CPTH$_2$*	
Atoms	**6-31G(d,p)**	**6-311(d,p)**	**6-31G(d,p)**	**6-311(d,p)**		**6-31G(d,p)**	**6-311(d,p)**	**6-31G(d,p)**	**6-311(d,p)**
	HOMO								
5C	7.41	7.3	5.66	5.86	5C	6.02	6.23	6.41	6.62
7S	38.46	38.18	43.71	42.63	7S	9.62	9.82	8.79	9.03
9O	5.13	4.93	3.93	3.97	9O	8.01	7.63	8.63	8.19
10C	6.34	6.25	4.75	4.95	10C	3.75	3.7	3.96	3.89
11C	3.74	3.72	-	-	12C	8.99	8.93	9.84	9.73
15C	6.62	6.58	4.94	5.2	15C	2.63	2.93	2.96	3.25
18C	6.98	7.09	5.57	5.88	16C	6.95	6.77	6.49	6.4
19N	-	-	4.1	3.65	17C	4.78	4.99	5.02	5.25
20N	11.70	11.76	8.42	8.93	18C	13.24	13.47	13.72	13.99
21N	3.25	3.13	2.38	2.43	20N	2.76	2.66	3.5	3.31
					21N	21.92	21.53	24.12	23.57

For the HOMO, the most contributions cause sulphur atoms of the thiosemicarbazone groups both for I4NPTH$_2$, I2-4DKPTH$_2$ ligands. The contributions of S7, and N20 belonging to thiosemicarbazone group, calculated with theory of B3LYP/6-311G (d,p) for I4NPTH$_2$, and I2-4DKPTH$_2$ are 38.18 %, 11.76%; and 42.63 %, and 8.93 %. The contribution of O9, belonging to indole ring of I4NPTH$_2$, and I2-4DKPTH$_2$ ligands was 4.93 %, and 3.97 %, respectively. The contributions of S7 and N20, belonging to thiosemicarbazone group, to LUMO was relatively low. They were 9.82 %, 2.66 %; 9.03 %, and 3.31%, respectively. The contributions of O9, belonging to indole ring was 7.63%, and 8.19 %.

A major contribution for LUMO belongs to N21 atom in the thiosemicarbazone group. The contributions of N21 atom for I4NPTH$_2$, and I2-4DKPTH$_2$ were 21.53%, and 23.57%, respectively.

Table-2: Theoretical and experimental ^{1}H-NMR chemical shift data for *I4NPTH$_2$*

Atoms	**Exp**	**6-31G (d,p)**	**6-311G (d,p)**	**6-311++G(d,p)**	**6-311G (2d,2p)**	**6-31G(d,p)-a**	**6-311G(d,p)-a**	**6-311++ G(d,p)-a**	**6-311 G(2d,2p)-a**
^{1}H-NMR									
H29	7.80	7.69	7.81	7.91	7.94	7.95	8.07	7.97	8.20
H24	6.96	6.75	6.87	6.82	7.02	7.28	7.42	7.18	7.57
H35	7.40	7.17	7.23	7.24	7.42	7.49	7.57	7.39	7.75
H25	7.10	7.38	7.47	7.35	7.59	7.77	7.89	7.60	8.02
H28	8.30	9.91	10.03	10.09	10.39	9.78	9.97	9.83	10.34
H23	8.30	6.71	6.88	6.97	7.11	7.33	7.48	7.38	7.70
H27	8.05	8.46	8.53	8.51	8.86	8.68	8.76	8.56	9.11
H22	8.05	8.40	8.43	8.53	8.78	8.69	8.74	8.70	9.09
H30	11.32	9.64	9.68	10.02	10.33	9.84	9.87	10.03	10.51
H31	13.00	12.84	12.59	12.92	13.37	13.20	12.91	12.90	13.60
H26	11.13	6.26	6.28	6.55	6.80	8.20	8.26	8.37	8.77
		0.769	0.760	0.797	0.794	0.813	0.801	0.834	0.826
^{13}C-NMR									
C17	122	116	126	127	126	118	128	129	128
C11	125	118	128	129	128	119	130	131	130
C5	137	126	137	137	137	129	141	141	140
C4	112	105	114	114	114	108	117	118	117
C10	142	137	148	149	149	140	151	152	151
C15	116	117	126	128	128	116	126	127	127
C18	133	125	133	134	134	131	139	141	140
C12	167	154	165	167	167	157	168	170	170
C16	183	171	181	183	182	172	183	186	184
C13	143	138	151	152	151	140	153	154	153
C3	124	114	122	123	122	117	127	128	127
C14		113	122	122	121	113	122	123	122
C1	126	120	130	131	131	122	133	134	133
C8		122	132	133	133	123	133	135	135
C2	146	140	152	153	152	140	152	152	151
		97.17	96.16	96.10	95.85	97.78	97.36	97.29	96.99

^{x} *indole*

3.3 NMR Studies:

The NMR chemical shifts of *I4NPTH$_2$ and I2-4CPTH$_2$* were obtained from RHF and DFT methods, employing the basis sets 6-31G (d,p), 6-311G (d,p), 6-311++G (d,p), 6-311G (2d,2p). On the otherhand and the NMR chemical shifts of Zn[(I4NPTH)$_2$] were obtained by employing the basis sets 6-311G (d,p) together with experimental values. The NMR chemical shifts of *I4IPTH$_2$, Zn[(I4IPTH)$_2$]* are presented in Tables-2-4. The ^{1}H-NMR chemical shifts correlation coefficient of *I4NPTH$_2$*, except indole hydrogen, was obtained from B3LYP method employing the basis sets 6-31G (d,p), 6-311G (d,p), 6-311++G (d,p) and 6-311++G (2d,2p) are δ 0.769, 0.760, 0.797, 0.794 for gas phase; and δ 0.813, 0.801, 0.834, 0.826, respectively, in DMSO.H$_3$0 and H25 chemical shifts were assigned as δ 11.32 and 13.00 as experimentally and δ 10.03 and 12.90 at the level of B3LYP/6-311++G (d,p) theory in DMSO for *I4NPTH$_2$*. N-H30 and N-H31 chemical shifts are assigned at δ 10.77 and 12.90 as experimentally and δ 10.36 and 12.63 at the level of B3LYP/6-311++G (d,p) theory in DMSO for *I2-4-CPTH$_2$*. N-H30 and N-H31 chemical shifts are assigned at δ 10.77 and 12.90 as experimentally and δ 10.36 and 12.63 at the level of B3LYP/6-311++G (d,p) theory in DMSO for *I2-4-CPTH$_2$*. The assignment of the peaks between δ 12.5-13.5 as the N-H31 is supported both by its location at lower field (indicative of an intramolecularly hydrogen-bonded proton) and by the greater dependency of its position on the nature of the N-H30 substituent.

In the ^{13}C-NMR spectra of isatin, C12, C18, C9 appeared at δ 159.4, 184.45 and 150.77. Upon formation of the TSC, the ketonic (now azomethine) carbon signal appeared at significantly higher field (*i.e.* δ 131.5-134.8). The exact position being dependent on the nature of the N12 substituent [23]. ^{13}C-NMR spectra of *I4NPTH$_2$, I2-4-CPTH$_2$*, and C12, Zn[(I4NPTH)$_2$] gives C12 at respectively, δ 167, 163, 172 and C10 at δ142, 143, 155.

Table-3: Theoretical and experimental ^{1}H-NMR data for *I2-4CPTH$_2$*

Atoms	Experimental	6-31 G(d.p)	6-311 G(d.p)	6-311++ G(d.p)	6-311 G(2d.2p)	6-31 G(d.p)-a	6-311 G(d.p)-a	6-311++ G(d.p)-a	6-311 G(2d.2p)-a
^{1}H-NMR									
H28	7.70	7.77	7.92	7.94	7.95	7.80	7.95	7.78	7.99
H24	6.95	6.71	6.84	6.78	6.98	7.27	7.42	7.17	7.55
H33	7.50	7.14	7.22	7.20	7.37	7.47	7.57	7.35	7.71
H25	7.62	7.33	7.44	7.31	7.55	7.76	7.88	7.56	7.99
H23	7.75	10.08	10.19	10.29	10.58	9.84	9.96	9.87	10.34
H22	7.10	7.14	7.29	7.34	7.51	7.58	7.74	7.58	7.93
H27	7.38	7.22	7.38	7.60	7.77	7.73	7.90	7.91	8.27
H29	10.77	10.15	10.15	10.45	10.91	10.23	10.24	10.36	11.01
H30	12.90	12.71	12.50	12.79	13.24	12.91	12.67	12.63	13.25
H26	11.27	6.21	6.25	6.53	6.76	8.18	8.25	8.35	8.74
R^2		0.824	0.806	0.815	0.826	0.873	0.858	0.860	0.866
^{13}C-NMR									
C17	121	117	127	127	127	118	111	128	127
C11	128	118	128	129	128	119	112	131	129
C5	133	126	137	136	136	129	122	140	140
C4	111	105	114	114	114	108	101	118	117
C10	143	137	148	148	149	139	132	151	151
C15	123	117	127	128	128	116	109	128	127
C18	132	125	132	134	133	131	124	140	139
C12	163	154	165	167	167	157	150	170	170
C16	178	171	181	183	182	171	164	185	183
C13		130	141	142	141	130	123	142	142
C3	120	114	124	125	124	115	108	126	124
C14	133	127	136	137	136	128	121	139	138
C1	129	123	133	134	133	124	117	135	134
C8	132	124	135	135	134	125	118	137	136
C2	135	133	143	144	143	134	126	144	143
R^2		0.988	0.985	0.988	0.986	0.982	0.986	0.993	0.994

3.4 UV Studies:

UV absorption data, along with calculated by TDB3LYP method and wavenumber and oscillator strength values for *I4NPTH$_2$, I2-4CPTH$_2$* are presented in Table-5. The electronic spectra of *I4NPTH$_2$, I2-4CPTH$_2$* showed absorption bands at 249 and 265 nm as experimental while theoretically obtained UV absorption spectra, calculated by TDDFT/6-311G(d,p) method, showed absorption at 250 and 261 nm. The absorption band at 250 nm of *I4NPTH$_2$* is seen due to transition mainly HOMO to LUMO+3 and HOMO to LUMO+4. HOMO consists of + 22.4%*10pz(S7)* + 8.1%*11pz(S7)* + 7.3%*9pz(S7)*- 5.3%*3pz(N20)*- 3.7% *4pz(N20)*+ 3.3%*3pz(C18),* to LUMO+3 and LUMO+4 consist of +12.3%*4pz(C4)*+ 11.7%*4pz(C17)*+ 10.1%*3pz(C4)*+ 9.9%*3pz(C17)*+ 5.7%*2pz(C4)*+ 5.6%*2pz(C17)* and + 12.5%*3pz(C16)*+ 7.4%*4pz(C16)*+ 7.1%*2pz(*C16)- 5.1% 11pz(S7)+ 4.8% 3pz(N32)- 4.6%10pz(S7).

Table-4: Theoretical and experimental ^{1}H-NMR data for *Zn[(I4NPTH)$_2$]*.

Atom	*I4IPTH$_2$*	*Zn[(I4IPTH)$_2$]*	*Zn[(I4NPTH)$_2$]*		
	Exp	Exp	Exp	6-31G(d,p)	6-311 G(d,p
H29	7.49(d)	7.02(d)	7.05	6.58	6.65
H24	6.93(d)	8.08	8.13	7.6	7.69
H35	7.09(t)	7.14(t)	7.44	7.21	7.29
H25	7.36(t)	7.38(t)	7.2	6.73	6.77
H28	7.75(d)	7.59(d)	8.3	6.6	6.87
H23	7.75(d)	7.59(d		8.35	8.4
H27	7.09(d)	7.74(d)	8.05	10.25	10.32
H22	7.09(d)	7.74(d)		8.69	8.71
H30	10.78(s)	10.68(s)	11.21	7.07	7.44
H31	12.84(s)				
H26(indole)	11.25(s)	11.06(s)	11.09	6.27	6.23
C17	128	125	125	120	130
C11	121	123	119	117	126
C5	132	132		128	139
C4	120	117	112	105	113
C10	143	142	155	137	148
C15	111	111	117	116	124
C18	133	137	166	142	151
C12	163	166	172	151	162
C16	176		183	173	183
C13	137	139	142	138	150
C3	122	124	122	118	128
C14	122	124		113	122
C1	138	137	137	123	133
C8	138	137		120	130
C2	90	88	146	139	152

The other absorption bands for *I4NPTH$_2$*, *I2-4CPTH$_2$* were observed at 365 and 368 nm, respectively as experimental while theoretically obtained UV absorption spectra, calculated by TDDFT/6-311G(d,p) method showed absorption at 358 and 357 nm. The absorption band at 365 nm of I4NPTH$_2$ was due to transition mainly between HOMO-3 to LUMO and HOMO to LUMO. HOMO-3 consits of - 7.1% 3pz(C4)+ 6.7% 3pz(N6) + 6.4% 3pz(C11) - 6.1% 4pz(C4) + 5.8% 4pz(C11)+ 5.3% 3pz(C17) and LUMO consist of+ 9.4% 3pz(N21)+ 6.8% 4pz(N21)+ 5.4% 2pz(N21)+ 5.2% 10pz(S7)- 5.2% 3pz(C18)- 5.0% 4pz(C18). The comparison between the experimental and theoretical values indicated that DFT/B3LYP method was in good agreement with the experimental data in predicting the UV absorption properties. The band at 360 nm in the UV-VIS spectrum of ligands was recorded in the range 415-449 nm.

Table-5: Experimental UV data, along with UV data calculated by B3LYP method wavenumber and oscillator strength values for *I4NPTH$_2$, I2-4CPTH$_2$,Zn[(I4NPTH)$_2$]*

I4NPTH$_2$			
Experimental	**365**	**249**	
6-31G(d,p)	358 [3.47(0.58) E5]	248[5.00(0.14) E18]	
6-311G(d,p)	358[3.47(0.56) E5]	250[4.97(0.18) E19]	
6-311++G(d,p)	364[3.41(0.45) E5]	254[4.88(0.14) E19]	
6-311++G(2d,2p)	364[3.40(0.47) E5]	265[4.88(0.12) E19]	
cep-31g*$^{(1)}$	339[3.66(0.56) E4]	239[5.18(0.18) E16]	
I2-4CPTH$_2$	**gaz**		
Experimental	**368**	**265**	
6-31G(d,p)	356 [3.48(0.51) E4]	259[4.78(0.25) E12]	
6-311G(d,p)	357[3.47(0.50) E4]	261[4.74(0.21) E12]	
6-311++G(d,p)	362[3.42(0.481) E4]	264[4.70(0.18) E12]	
6-311++G(2d,2p)	363[3.41(0.48) E4]	265[4.68(0.16) E12]	
cep-31g*$^{(1)}$	338[3.66(0.43) E4]	246 [5.03(0.18) E12]	
Zn[(I4NPTH)$_2$]			
Experimental	**449**	**318**	**258**
6-31G(d,p)	445 [2.78(0.33) E7]	312 [3.97(0.37) E29]	256[4.84(0.08) E67]
6-311G(d,p)	469 [2.64(0.24) E3]	312 [3.97(0.37) E29]	258 [4.83(0.11) E68]

3.5 IR Studies:

The frequency scale is presented in units of reciprocal centimeters (cm^{-1}). Absorption bands in the 4,000 to 1,450 cm^{-1} regions are usually due to stretching vibrations of diatomic units, which is sometimes called frequency region. In this study, 4000 to 1250 cm^{-1} region was studied with B3LYP/ 6-311G (d,p) and was given in Table-3. There are nitrogen and oxygen donor atoms in isatin ring, and nitrogen and sulphur donor atoms in isatin thiosemicarbazones.

In the IR spectra of *I4NPTH*$_2$, *I2-4CPTH*$_2$, and Zn[(I4NPTH)$_2$] NH the stretching vibrations due to indole ring were at 3281, 3255 and 3291 cm^{-1}. Two bands at 3173 to 3156 cm^{-1} for *I4NPTH*$_2$, and 3173 to 3149 cm^{-1} were attributed to the ν(NH) of the thiosemicarbazonic chain, but in the Zn[(I4NPTH)$_2$] complex only one band, belonging to N19 atom, at 3150 cm^{-1} was detected. Compounds *I4NPTH*$_2$, *I2-4CPTH*$_2$ and Zn[(I4NPTH)$_2$] showed absorption bands at 1693, 1690 and 1696cm^{-1} resulting from the C=O function of indole ring. The band at 1696 cm^{-1} in the Zn[(I4NPTH)$_2$] complex supported the uncoordinated to CO group. Infrared spectra of the *I4NPTH*$_2$ ligand showed bands at 1624 and 1514 cm^{-1}, assigned to the ν (C18=N21) and δ(N20H), vibrations, respectively. In complex, these bands disappeared indicated that the coordination takes place through the nitrogen atom and deprotonation occurs during the coordination.

Table-6: Experimental IR data of *I4NPTH*$_2$, *I2-4CPTH*$_2$ and Zn[(I4NPTH)$_2$]

***I4NPTH*$_2$**			***I2-4CPTH*$_2$**			**Zn[(I4NPTH)$_2$]**			**Tentative Assignment**
Exp	*Freq*		*Exp*	*Freq*		*Exp*	*Freq*		
3281	3642	80	3255	3643	77	3291	3646	152	υ (N6H)
3173	3494	133	3173	3466	115	3150	3600	172	υ (N19H)
3156	3421	104	3149	3425	99				υ (N20H)
3115	3242	10	3075	3228	24	3078	3243	157	υ (C8H), υ(C14H)
3068	3200	15	3027	3199	14		3200	19	υ (CH)ringB
2834	3190	14	2834	3191	14	2977	3189	11	υ (CH) ringB
1693	1777	242	1690	1776	242				υ (C12-O9), δ (N20H), δ (N6H), υ (C18-N21), δ (N19H)
						1696	1798	602	υ (C12-O9), δ (N6H)
1624	1663	117	1619	1663	110				υ (CC) ringB, δ (CH) ringB, δ (N6H), υ (C18-N21), δ (N6H), δ (N19H), δ (N20H)
						1603	1662	232	υ (CC) ringB, δ (CH) ringB, δ (N6H),
1598	1654	71					1651	154	υ (CC)ringA δ (CH)ringA, δ (N19H), υ (ONO), υ (C16-N19)
1538	1643	118				1538	1639	138	υ (CC)ringA, δ (CH)ringA, υ (NO), υ (C16-N19), δ (N19H),
	1637	29	1579	1637	90		1631	23	υ (CC)ringB, δ (CH)ringB, υ (C18-N21), δ (N6H)
			1526	1634	97				δ (N19H), υ (N19C13), υ (CC) ringA, δ (CH) ringA, υ (CC)ringB, υ (C18-N21)
1514	1628	90	1490	1628	106				υ (C18N21), δ (N20H), δ (N6H), υ (CC)ringB, δ (CH) ringB
			1476	1619	328				δ (N19H), υ (CC) ringA, (CH) ringA
1493	1611	769				1495	1604	408	δ (N19H), υ (CC) ringA, (CH) ringA, υ (ONO)
						1457	1598	217	υ (C18N21), υ (C16N20), υ (N19H)
1461	1578	402					1568	19	δ (N19H), υ (CC) ringA, υ (ONO), υ (C16-N19)
						1427	1565	663	δ (N19H), υ (CC) ringA, υ (C16-N19), υ (ONO)
			1455	1570	716				δ (N19H), υ (CC) ringA , δ (N20H), υ (C16-N19)
1408	1531	103	1415	1528	199				δ (N20H), δ (CH) ringB δ (CH) ringA, δ(N19H)
1372	1525	182							δ(CH) ringA,δ(N19H)) ringB, δ(CH) ringA, δ(N20H)
						1389	1524	158	δ (CH) ringA, δ (N19H)) ringB, δ (CH) ringA
							1517	19	υ (CH) ringB, δ (N6H)
1335	1513	18	1369	1514	13				δ (CH)ringB, δ (N20H), δ (N6H)
						1352	1499	181	δ (CH) ringB
			1338	1497	89				δ (CH)ringA ,δ (CH)ringB, δ (N19H)
1303	1495	133							δ (CH) ringB , δ (N20H)
			1298	1492	120				δ (CH)ringA , δ (CH)ringB, δ (N20H)
						1315	1463	681	δ (CH) ringA, υ (N20C16), υ (NO)
						1300	1461	772	δ (CH) ringA, υ (N20C16), υ (NO)
						1255	1433	1595	δ (CH) ringA, υ (N20C16N19)
						1245	1420	14848	υ (CC) ringB, δ (CH) ring B, δ (N6H)
1274	1417	74							υ (CC) ringB, δ (CH) ring B, δ (N6H), υ (C16N19)
			1270	1416	95				υ (CC) ringB, δ (CH) ring B, δ (N6H), δ (CH) ring A, υ (C16N19)
1258	1393	253							υ (N20C16N19), δ (NH)mol, υ (ONO), υ (C16S), υ (C16S)
			1240	1386	391				υ (N20C16N19), δ (NH)mol, υ (ONO)
						1227	1374	656	υ (CC) ringA, δ (CH) ringA, υ (ONO), δ (N19H)

3.6 Anti-Glycation Activity

The formation of AGEs is a complex process, involving a variety of chemical reactions, mediated without the help of any enzyme. This initial stage of glycation results in the production of Schiff bases. In the middle stage, the rearrangement of Schiff base results in the formation of Amadori products. The Amadori products go through further rearrangement, dehydration, condensation, and addition reactions with other proteins. This irreversible series of reactions finally leads to the formation and accumulation complex array of advanced glycation endproducts (AGEs). It is therefore possible to inhibit the AGE formation *in vitro* and *in vivo* through diverse interventions (e.g. antioxidants, transition metal ion chelators, AGE Receptor blockers, Anti-AGE antibodies, etc.) [24]. Additionally it is reported that multifunctional agents, such as carbonyl scavenging, metal ion chelating, and antioxidant activities within the same molecule may also effectively inhibit the glycation reaction.

A close examination of the basic skeleton of metal derivatives of isatin-3-thiosemicarbazones, with different functionalities such as thiourea, oxindole, and transition metal (Zn or Ni) indicate that these compounds can exert their biological potential through multitude of way. The anti-glycation prperties of both amine and thiol groups in cross-link formation is well studied. Therefore thiol group containing molecules can be facile target of glycation. On the basis of these findings, thiols or other sulfur-containing compounds (such as *N*-acetylcysteine, homocysteine, thiourea, etc.) can act as competitive nucleophiles to react with reducing sugars and dicarbonyls, thus prevent the non-enzymatic protein glycation reaction [25].

Compounds **1**-**12** contain thiourea group, along with amino group in the proximity. Hence the observed anti-glycation activity of these compounds may be due to the interaction of sulfur atom with methylglyoxal, thereby preventing the glycation reaction. However, based on the limited number of compounds, only a superficial understanding about the structure-activity relationship could be developed. Among the different non-metal chelated derivatives of isatin-3-thiosamicarbazones, compounds **1**- **4** were found to be largely inactive with 24.37, 24.84, 24.94 and 45.45 % inhibition, respectively. While metal chelated analogs, i.e. compound **8** (IC_{50} = 111.30 ± 1.96 µM), and **10** (IC_{50} = 113.00 ± 0.9 µM) showed potent anti-glycation potential, as compared to the standard, i.e. rutin (IC_{50} = 294.5 ± 1.5 µM). These compounds have same structural features, except metal atom. Compound **8** has "Ni", while compound **10** possess "Co" atoms. Results showed that when isatin-3-thiosamicarbazones have Ni metal, they exhibit potent activity such as compound **8** (IC_{50} = 111.30 ± 1.96 µM), than Co containing isatin-3-thiosamicarbazones, as is the case with compound **8** and **10**. Ni containing isatin-3-thiosamicarbazones derivatives were also found to be more potent than the Zn containing isatin-3-thiosamicarbazones analogs, as is the case with compounds **7** and **11**. Compound **7** (IC_{50} = 271.16 ± 5.8 µM) bears Zn metal, while **11** (IC_{50} = 247.55 ± 1.57 µM) have Ni atom in its core. To observe the effect of different substituents, we compared the antiglycation activity of compounds **8**, **9**, **11**, and **12**. These compounds have same structural features, even the same metal atom (i.e. Ni), but possess different substituents at benzene ring. Compound **8** have a *p*-nitro benzene moiety (IC_{50} = 111.30 ± 1.96 µM) and showed more potent antiglycation activity than compounds **9** (IC_{50} = 137.78 ± 2.43 µM), **12** (IC_{50} = 185.72± 3.18 µM), and **11** (IC_{50} = 247.55 ± 1.57 µM). Compound **9** have a *p*-iodobenzene group, compound **12** possess *p*-fluorobenzene moiety, while compound **11** have *o*,*p*-dichlorobenzene group in its skeleton. From these results, we can conclude that nitro group is crucial to inhibit the process of protein glycation more effectively, than the other electron donating groups (*i.e.* iodo, flouro and chloro).

Table-7: *In vitro* anti-glycation activity of compounds 1-12

Compound	Structure/IUPAC Name	IC_{50} ± SEM[1] (µM)
1	1*H*-İndole-2,3-dione 3-(4 nitrophenyl)thiosemicarbazone	NA[2]
2	1*H*-İndole-2,3-dione-3-(4 iodophenyl)thiosemicarbazone	NA[2]
3	1*H*-İndole-2,3-dione-3-(2,4dichlorophenyl)thiosemicarbazone	NA[2]
4	Isatin-3-(4-chlorophenyl)thiosemicarbazone (II)[4]	NA[2]
5	*Bis*(isatin-3-(4-nitrophenyl)thiosemicarbazonato)zinc (II)	161.51 ± 0.47
6	*Bis*(isatin-3-(4-iodophenyl)thiosemicarbazonato)zinc (II)	224.40 ± 1.00
7	*Bis*(isatin-3-(2,4-dichlorophenyl)thiosemicarbazonato)zinc (II)	271.16 ± 5.8
8	*Bis*(isatin-3-(4-nitrophenyl)thiosemicarbazonato)nickel (II)	111.30 ± 1.96
9	*Bis*(isatin-3-(4- iodophenyl)thiosemicarbazonato)nickel (II)	137.78 ± 2.43
10	*Bis*(isatin-3-(4-nitrophenyl)thiosemicarbazonato)cobalt (II)	113.00 ± 0.9
11	*Bis*(isatin-3-(2,4-dichlorophenyl)thiosemicarbazonato) nickel (II)	247.55 ± 1.57
12	*Bis*(isatin-3-(2- florophenyl)thiosemicarbazonato)nickel (II)	185.72 ± 3.18
Standard	Rutin	294.50 ± 1.5

[1] *IC_{50} Values are expressed as mean ± standard error of mean*
[2] *NA: Not Active*
[3] *{26]*

CONCLUSION

$Zn[(I4NPTH)_2]$, $Zn[(I4IPTH)_2]$, $Zn[(I2\text{-}4CPTH)_2]$, $Ni[(I4NPTH)_2]$, $Ni[(I4IPTH)_2]$, $Co[(I4NPTH)_2]$, $Ni[(I2\text{-}4CPTH)_2]$, $Ni[(I2FPTH)_2]$, were synthesized and structually characterized. Vibrational frequencies and intensities were calculated at the level of theor B3LYP/6-311G(d,p). ^{1}H-NMR and ^{13}C-NMR calculations and UV absorption calculations were also carried out with B3LYP method and compared with the experimental data. Fukui functions of *$I4NPTH_2$,$I2\text{-}4CPTH_2$* ligands were calculated by using AOMix program. The contributions of S7, N20, belonging to thiosemicarbazone group were calculated with B3LYP/6-311G(d,p) for I4NPTH2 and found to be 38.18 %, 11.76; and 42.63 % and 8.93 %, respectively. The contributions of S7, program N20, belonging to thiosemicarbazone group were calculated with theory of B3LYP/6-311G(d,p) for I4NPTH2 are 38.18 %, 11.76; and 42.63 % and 8.93 %.

On the basis results, it may be inferred that in isatin, and their metal complexes (*i.e.* compounds **1**-**12**) the presence of thiourea moiety, chelation with different metals and presence of different substituents at the main skeleton may all contributes towards their protein antiglycation activity.

Acknowledgements
The authors are grateful to the Nigde University Scientific Research Projects Unit (NUBAP, Project Number: FEB 2011/01) for their financial support during this study. Saima Rasheed also acknowledges Higher Education Commission, Pakistan, for financial support through "Indigenous 5000 Scholarship Programme, Batch-VII".

REFERENCES

[1] Medvedev A. E; Clow A; Sandler M; Glover V. *Biochem. Pharmacol*., **1996**, 52, 385-391.
[2] Sridhar S.K; Atmakuru R. *Indian Drugs*, **2001**, 38, 174-180.
[3] Pandeya S. N; Sriram D. *Acta Pharm. Turc*., **1998**, 40, 33-38
[4] Varma R.S; Nobles W.L. *J. Pharm. Sci*., **1975**, 64, 881-882.
[5] Pandeya S.N; Yogeeswari P; Sriram D; De Clercq E; Pannecouque C; Witvrouw M. *Chemotherapy*, **1999**, 45, 192-196.
[6] David C; Marie T; Roussel G; U.S. Pat. 5, 498, 716 (**1996**) [*Chem. Abstr*., 124, 343271 (1996)].
[7] Pandeya, S. N.; Sriram, D.; Nath, G.; De Clercq, E.; *Pharm. Acta Helv.*, **1999**, 74, 11-17.
[8] Imam S.A; Varma R. S. *Experientia.*, **1975**, 31, 1287-1288.
[9] Karali N; Gursoy A; Kandemirli F; Shvets N; Kaynak F.B; S. Ozbey V.K; and Dimoglo A. *Bioorganic and Medicinal Chemistry*, **2007,** 15, 5888-5904.
[10] Cerchiaro G; Ferreira A.C. *Journal of the Brazilian Chemical Society*, **2006,** 17, 1473-1485.
[11] Gunesdogdu-Sagdinc S; Köksoy B; Kandemirli F; Bayari S.H. *J. Mol. Struct*., **2009**, 917, 63-70.
[12] Kandemirli F; Arslan T; Karadayı N; Ebenso E.E; Koksoy B. *J. Mol Struct*., **2009**, 938, 89-96.
[13] Kandemirli F; Arslan, T; Koksoy, B.; Yılmaz M. *J. Chem. Soc. Pak*., **2009**, 31, 498-504.
[14] Choudhary I; Siddiq S, Saracoglu M, Hakan Sayiner H., Arslan Erbay A., and Köksoy Quantum Chemistry-Molecules for Innovations, Part 2, Chapter 3: Quantum chemical calculations for some isatin thiosemicarbazones, ISBN 978-953-51-0372-1, InTech - Open Access Publisher,pp 25-58, March **2012**
[15] Kandemirli F; Koksoy, B; Arslan T; Sagdınc S; Berber H. *Journal of Molecular Structure*, **2009**, 921, 172-177
[16] Gorelsky S.I. AOMix: Program for Molecular Orbital Analysis; University of Ottawa, **2009**, http://www.sg-chem.net/
[17] Gorelsky S.I; Lever A.B.P. *J. Organomet. Che*m., **2001**, 635, 187-196.
[18] Lee C; Yang W; Parr R.G. Phys Rev B., **1988**, 37, 785-789.
[19] Ulrich P; Cerami A; Protein Glycation, Diabetes, and Aging, **2001**, *Recent Progress in Hormone Research*, 56, 1-21.
[20] Gaussian 09, Revision B.1, Frisch M.J; Trucks G.W; Schlegel H.B; Scuseria G.E; Robb M. A; et all,. Gaussian, Inc., Wallingford CT, **2010**.
[21] Choudhary M.I; Ali M; Wahab A; Khan A; Rasheed S; Shyaula S.L; Rahman A.U., *Sci. China Chem.*, **201**1, 54 (12), **1926-1931**.
[22] Zeb A; Malik I; Rasheed S; Choudhary M.I; Basha F.Z. *Med. Chem*, **2012**, 8, 846-852.
[23] Bain G.A; West D.X; Krejci J; Martinez J.V; Ortega S.H; and Toscano R.A. *Polyhedron.*, **1997**, 16, 855-862.
[24] Rahbar S; Figarola J.L. *Archives of Biochemistry and Biophysics.*, **2003** 419, 63–79,.
[25] Zeng J; Dunlop R. A.; Rodgers K. J; Davies M. J. *Biochem J*., **2006**, 398(Pt 2), 197–206.